Supporting Information

for

Cu(II)/Fe(II) Electron-Deficient Pairs as Bifunctional Catalysts for Efficient PMS Activation and Solar-Driven Water Evaporation

Wanyu Zhang[1,a], Xixing Wang[1,a], Danhong Shang[a], Linzhi Zhai[a], Xiaobo Zhang[c,*], Fu Yang [a,*], Edison Huixiang Ang[b,*]

[a] *School of Environmental and Chemical Engineering, Jiangsu University of Science and Technology, Zhenjiang 212100, Jiangsu, China*

[b] *Natural Sciences and Science Education, National Institute of Education, Nanyang Technological University Singapore, 637616, Singapore*

[c] *Department of Radiology, First Medical Center, Chinese People's Liberation Army General Hospital, Beijing, China*

1 equal contribution

* *Corresponding author: E-mail:* Prof. Fu Yang, *fuyang@just.edu.cn*; Xiaobo Zhang, *zhangxiaobo301@126.com*; Edison Huixiang Ang, *edison.ang@nie.edu.sg.*

Text S1. Comprehensive testing of degradation

The 20 mg L^{-1} TC solutions were prepared to simulate a contaminant system and were posed to achieve a homogeneous mixture. In each experiment, 10 mg of persulfate (PMS) oxidant was added to 50 mL of the simulated composite pollutant solution and sonicated to ensure uniform dissolution (initial 1-minute ultrasonic treatment followed by mechanical stirring). Subsequently, the prepared catalyst sample was uniformly dispersed in the solution at a concentration of 0.2 g L^{-1} to initiate both degradation and adsorption processes, which were accompanied by continuous mechanical stirring at 400 rpm. At specified time intervals, aliquots of the reaction solution were withdrawn from the reactor, immediately filtered through a 0.45 μm nylon membrane, and analyzed for dynamic concentration monitoring of TC using ultraviolet-visible (UV-Vis) spectrophotometry, high-performance liquid chromatography (HPLC), and inductively coupled plasma mass spectrometry (ICP-MS).

Text S2. The parameters of HPLC used for TC degradation

Chromatographic column: Phenomenex Gemini C18 column (250 mm × 4.6 mm, 5 μm)

Mobile phase: A mixture of 0.1% formic acid aqueous solution (A) and acetonitrile (B)

Elution program: Isocratic elution, A:B = 87:13 (volume ratio)

Flow rate: 0.4 mL/min

Column temperature: 40 °C

Detection wavelength: 355 nm

Text S3. Confirmation of highly toxic intermediates and discussion on potential ecological impacts

Aquatic toxicity analysis

P2 (m/z = 459): The molecular weight is larger than TC, but the structural change may cause its toxicity to specific aquatic organisms (such as green algae) to exceed that of TC.

P13 (m/z = 405): The molecular weight is still large, but the structural change may cause its toxicity to green algae to exceed that of TC.

Developmental toxicity analysis

P5 (m/z = 120): As above, its structural change may endow it with characteristics similar to those of environmental endocrine disruptors, thereby having higher developmental toxicity than TC.

P10 (m/z = 182): These are intermediates with significant structural alterations but not completely fragmented. They may retain some of the biological activities of the TC parent nucleus, and due to structural distortion, they have a stronger binding ability to development-related receptors, thus resulting in higher developmental toxicity.

Mutagenicity analysis

P13 (m/z = 405): Polycyclic conjugated compounds bearing multiple carbonyl and phenolic groups are well-recognized mutagenic scaffolds. Their planar structures and highly reactive electrophilic sites facilitate direct interactions with DNA, including intercalation and covalent adduct formation, leading to a high predicted mutagenic potential.

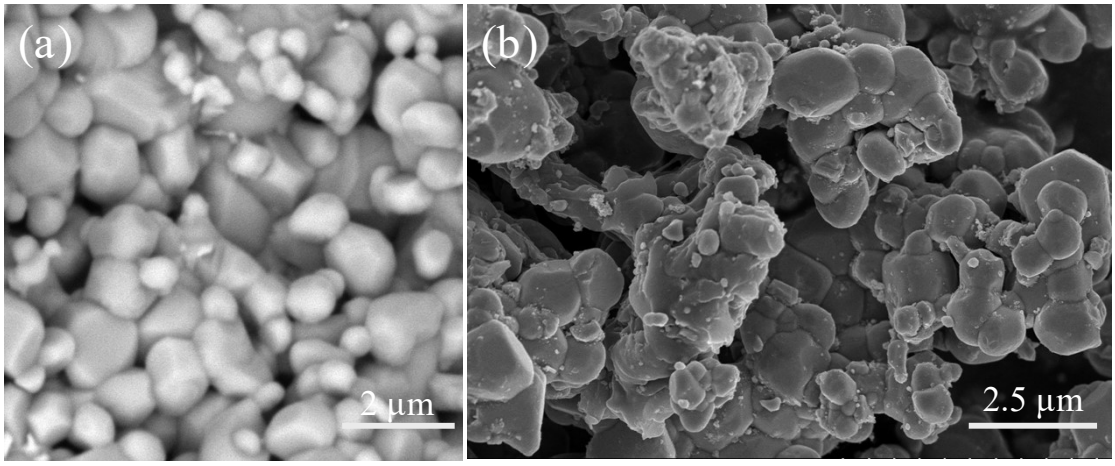

Fig.S1 SEM images of Fe_3O_4-800 (a), and Fe/Cu-800 (b)

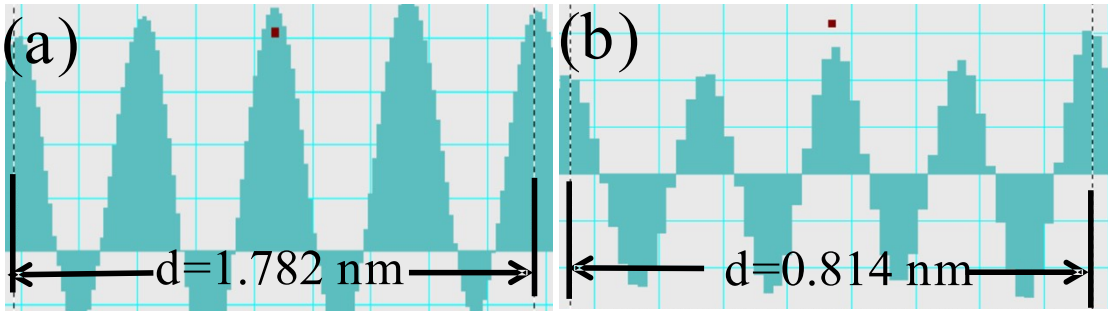

Fig.S2 (a) FeO (400), (b) Cu (111) planes in Fe/Cu-800 extracted from Fast Fourier Transform

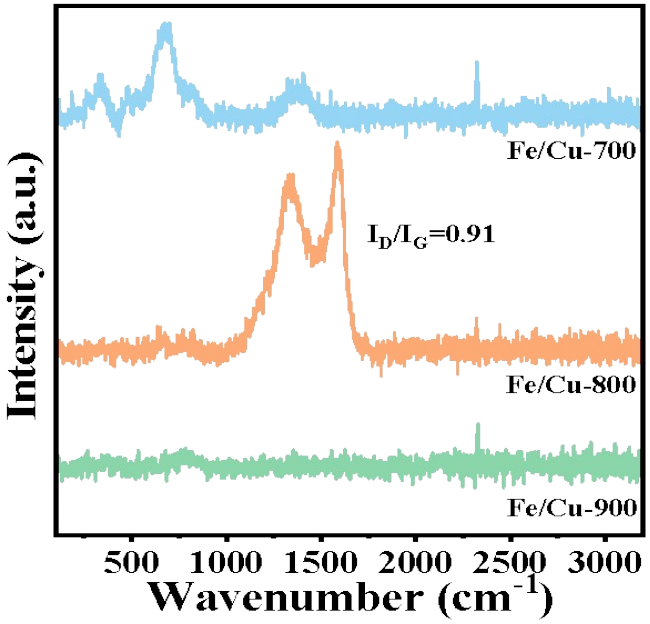

Fig S3. Raman spectra of Fe/Cu-700, Fe/Cu-800, and Fe/Cu-900.

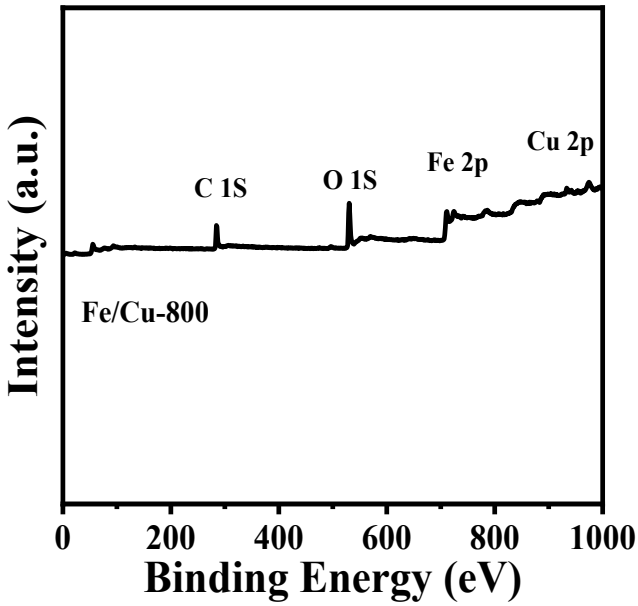

Fig S4. X-ray photoelectron spectroscopy spectra of Survey core levels in Fe/Cu-800.

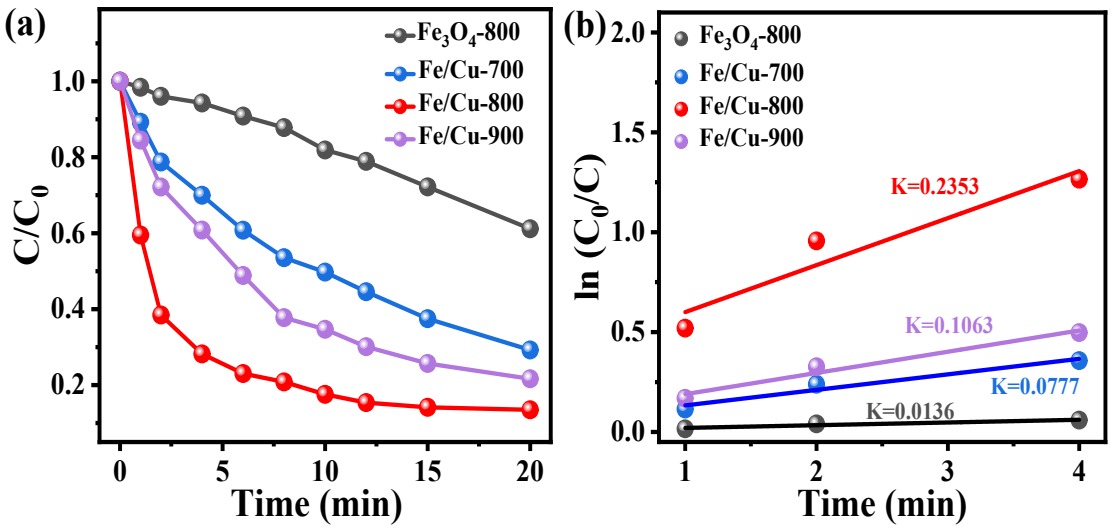

Fig S5. Time-dependent catalytic degradation course curves of TC on Fe_3O_4-800, Fe/Cu-700, Fe/Cu-800, and Fe/Cu-900 samples: (a) relationship between C/C_0 and reaction time, and (b) reaction rate.

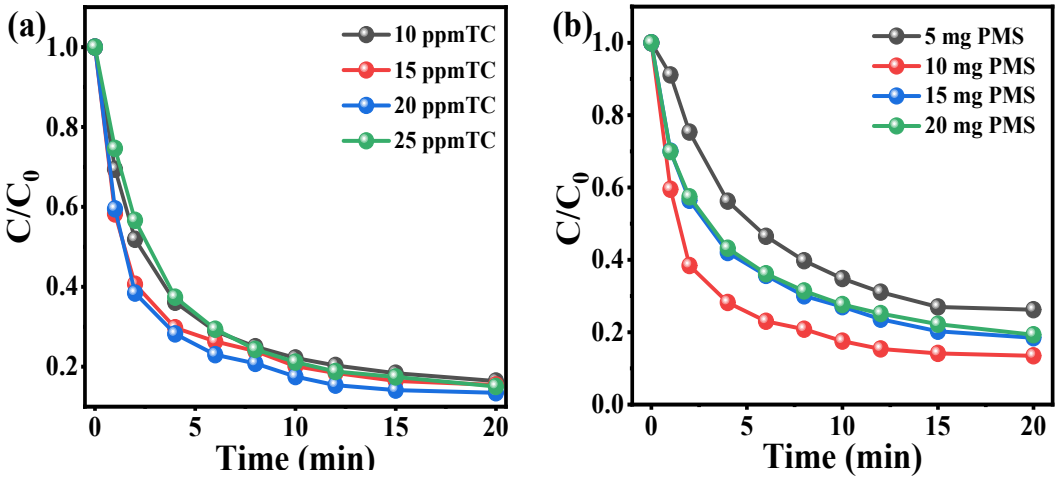

Fig S6. (a) Time-dependent TC degradation course curves over Fe/Cu-800 using different TC concentrations. Reaction condition: [catalyst] = 0.2 g L^{-1}, [PMS] = 0.2 g L^{-1}. (b) Time-dependent TC degradation course curves over Fe/Cu-800 using different PMS dosages. Reaction condition: [TC] = 20 mg L^{-1}, [catalyst] = 0.2 g L^{-1}.

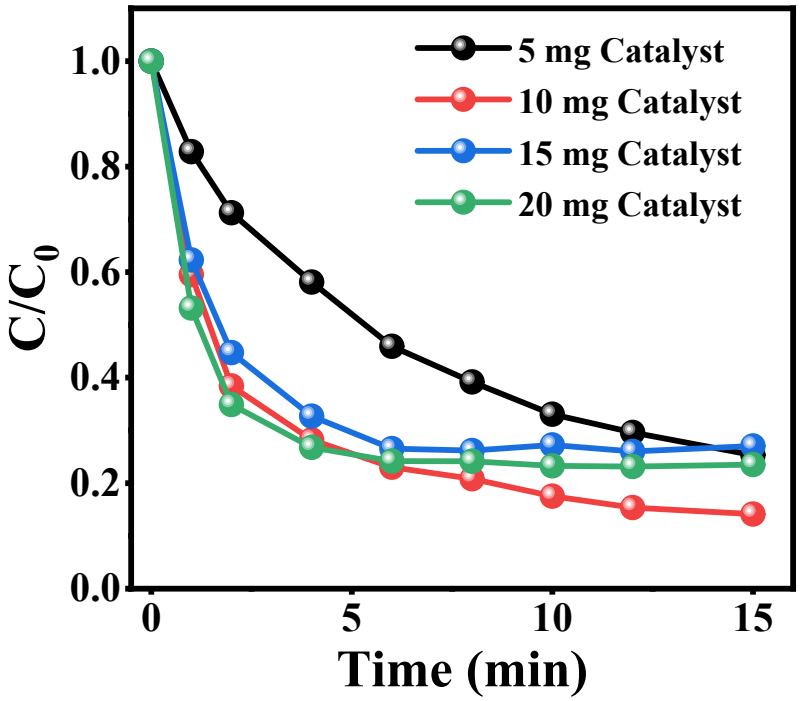

Fig S7. (a) Time-dependent TC degradation course curves over Fe/Cu-800 using different catalyst dosages. Reaction condition: [TC] = 20 mg L^{-1}, [PMS] = 0.2 g L^{-1}.

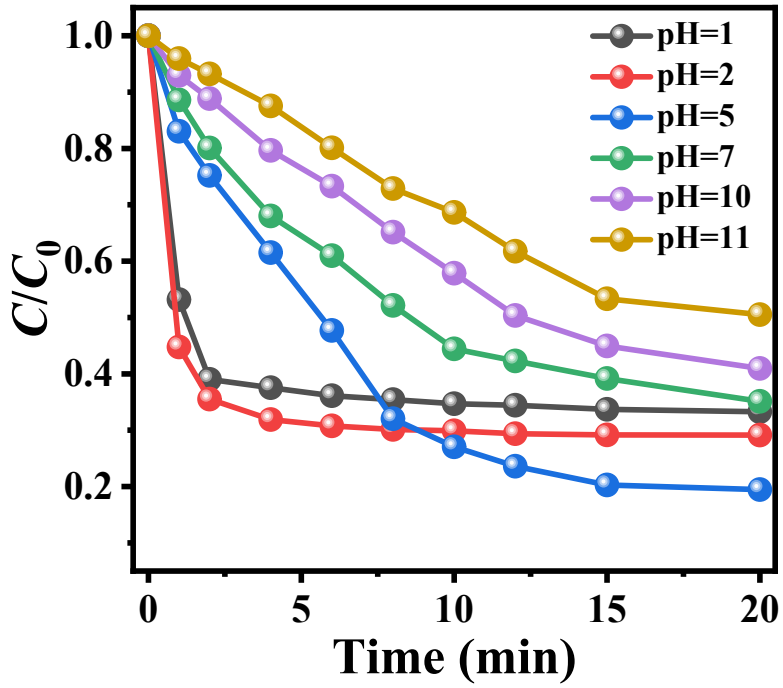

Fig S8. (a) Time-dependent TC degradation course curves over Fe/Cu-800 at different reaction pH tures. Reaction condition : [TC] = 20 mg L^{-1}, [PMS] = 0.2 g L^{-1}, [catalyst] = 0.2 g L^{-1}.

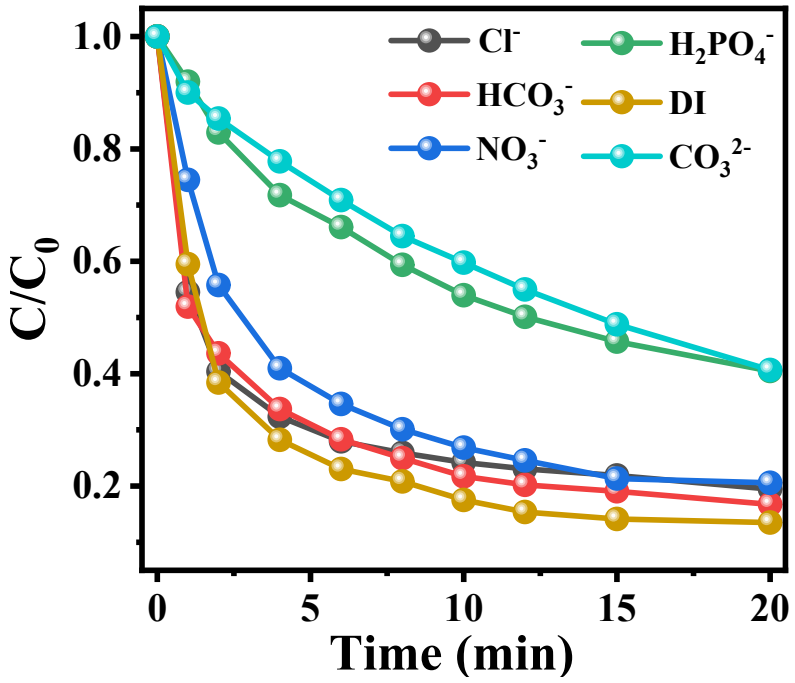

Fig S9. Time-dependent TC degradation course curves over Fe/Cu-800 with different anionic interferents.

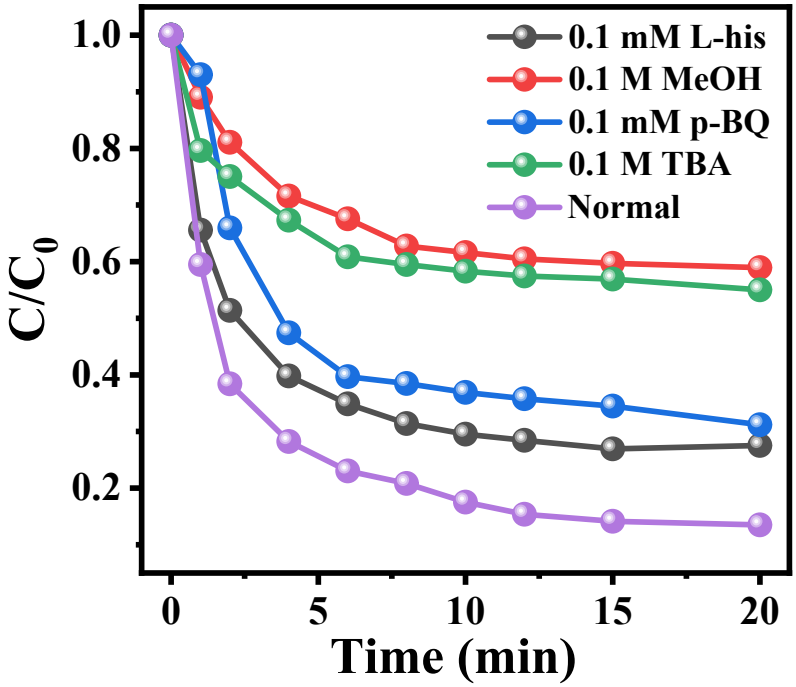

Fig S10. Effect of quenching agents of L-his, MeOH, P-BQ, TBA on TC degradation in the Fe/Cu-800/PMS system.

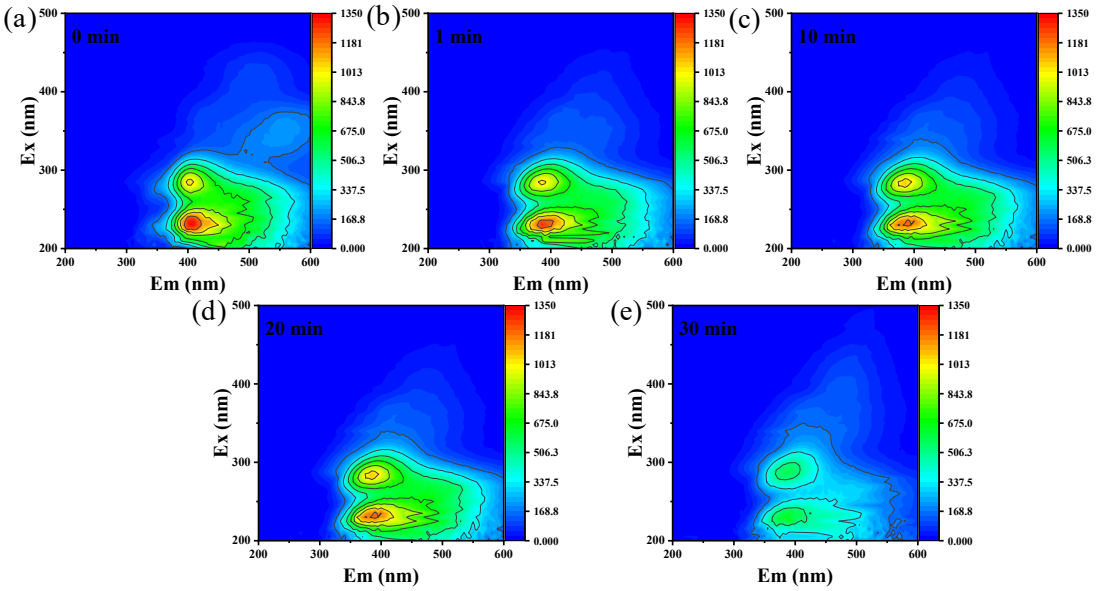

Fig S11. (a-e) 3D fluorescence spectrum condition: spectra during TC degradation process with Fe/Cu-800.Experimental conditions: [TC] = 20 mg L^{-1}, [PMS] = 0.2 g L^{-1}, [Catalyst] = 0.2 g L^{-1}.

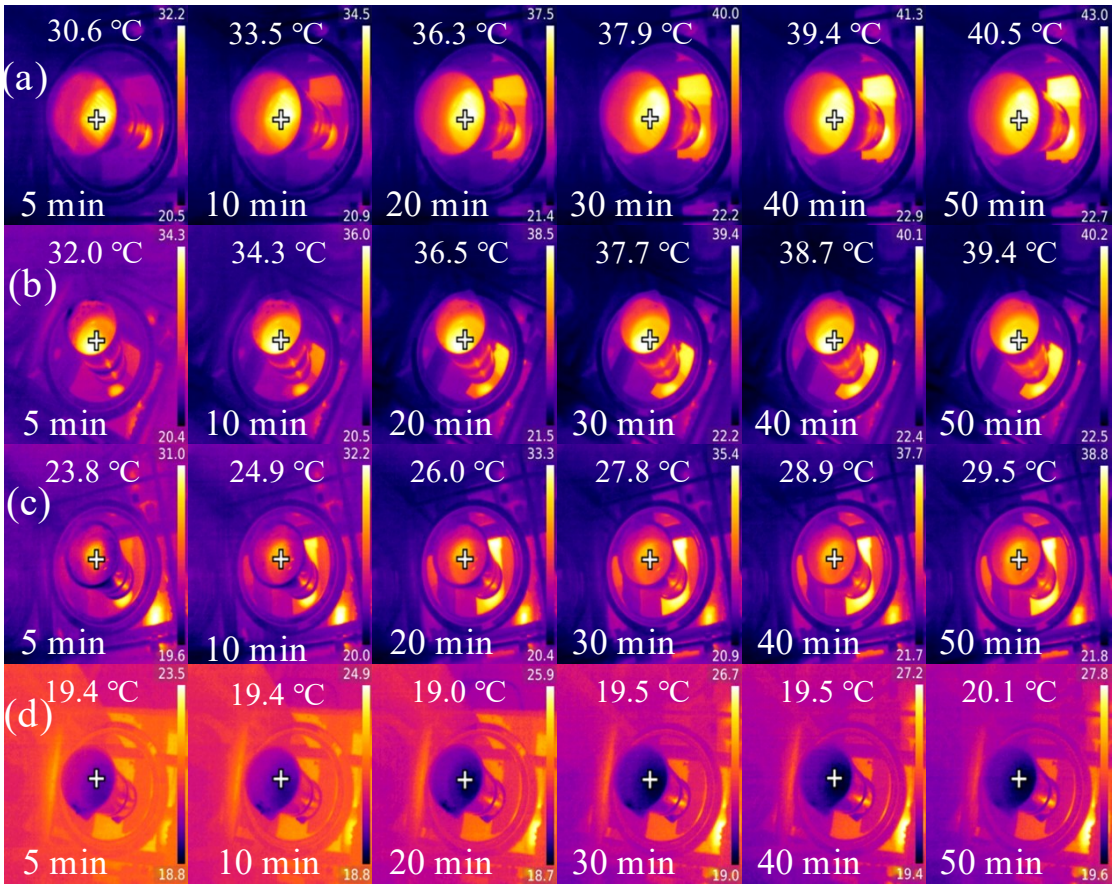

Fig S12. (a) Infrared thermal images of Fe/Cu-800 modified glass fiber evaporating tetracycline solution under illumination; (b) Infrared thermal images of Fe/Cu-800 modified glass fiber evaporating deionized water under illumination; (c) Infrared thermal image of glass fiber evaporating deionized water under illumination; (d) Infrared thermal image of Fe/Cu-800 glass fiber evaporating deionized water without illumination.

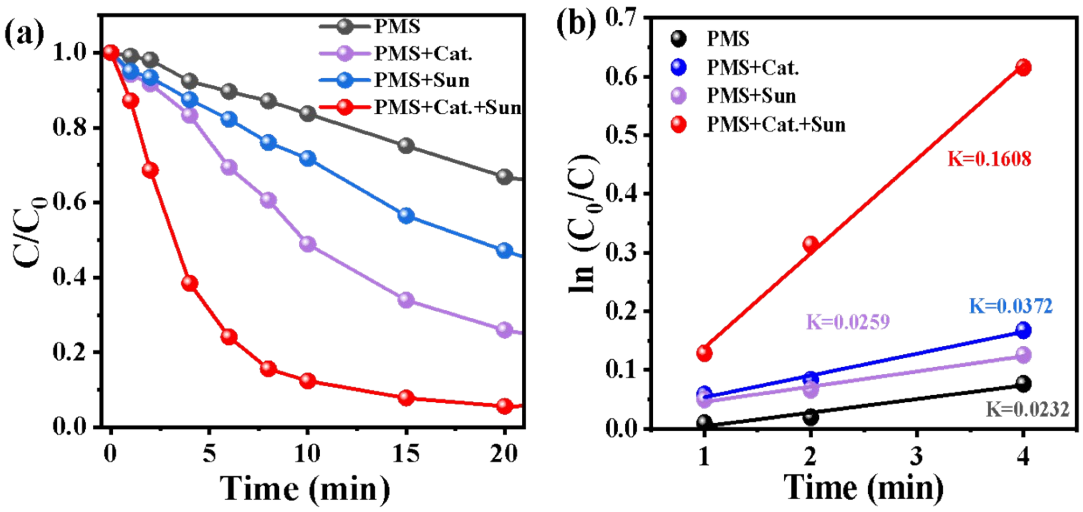

Fig. S13. The time-dependent catalytic degradation process curve of TC on the Fe/Cu-800 integrated evaporator: (a) the relationship between C/C_0 and reaction time, and (b) reaction rate.

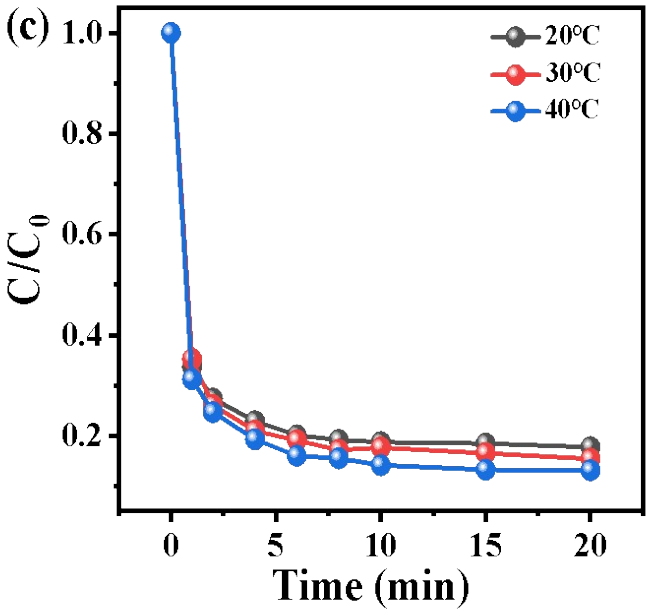

Fig. S14. The time-dependent TC degradation process curves of Fe/Cu-800 materials were studied at different temperatures.

Table S1. A summary of TC degradation performances in different heterogeneous catalyst/PMS systems.

Catalyst (g L^{-1})	PMS (mM)	TC (mg L^{-1})	Removal efficiency	k_{obs} (min^{-1})	k-value ($min^{-1}\cdot mM^{-1}$)	Ref.
Fe/Cu-800	**1.314**	**20**	**86.5% (20min)**	**0.235**	**0.179**	**This work**
Fe/Cu-700	1.314	20	70.8% (20min)	0.078	0.059	compare
Fe/Cu-900	1.314	20	78.4% (20min)	0.106	0.081	compare
Cu/MIL-101 (Fe)	8	300	89% (30min)	0.111	0.0139	[1]
FTO-2Co	1.314	10	81.2%	0.03	0.023	[2]
BC_{350}/Fe	0.6	20	85.26% (30min)	0.085	0.142	[3]
CoP@Co_2 P -3/	5.256	20	84.7% (14min)	0.248	0.047	[4]
Fe_3O_4@MC	2.628	25	75.90% (90min)	0.032	0.012	[5]
Fe_3O_4@T-BC	6.57	50	97.89% (60min)	0.023	0.003	[6]
Fe-O-BC	5	90	100% (40min)	0.123	0.025	[7]
10%WO_3/diatomite	3	40	80.75% (180min)	0.042	0.005	[8]
PC_3 N_4	6	20	81.75% (60min)	0.056	0.009	[9]
$Mn_{0.85}$ $Fe_{2.15}$ O_4 -CNTs	0.8	20	94.90% (60min)	0.071	0.089	[10]
Co Ni LDO/PMS	1.6	30	100% (60min)	0.16	0.1	[11]
0.5-MoS_2/$NiCo_2S_4$	2.628	15	98.20% (90min)	0.041	0.016	[12]
US/PMS	0.2	20	80.40% (60min)	0.018	0.090	[13]

Table S2. The influence of different inorganic anions on the corresponding TC concentration changes over time.

Time	Control	Cl^-	HCO_3^-	NO_3^-	$H_2PO_4^-$	CO_3^{2-}
0	1	1	1	1	1	1
1	0.59492	0.54505	0.51922	0.74496	0.91967	0.90021
2	0.38426	0.40375	0.43601	0.55784	0.82935	0.85408
4	0.28209	0.32349	0.33691	0.40959	0.71756	0.77772
6	0.23014	0.27946	0.28306	0.34616	0.66082	0.70905
8	0.20817	0.25894	0.24953	0.30094	0.59362	0.64467
10	0.17532	0.24199	0.21716	0.26842	0.53943	0.59764
15	0.14133	0.2188	0.19052	0.21334	0.45696	0.48784
20	0.13486	0.19462	0.16729	0.20574	0.40473	0.40647

Table S3. ICP-OES elemental analysis of Fe and Cu content in Fe/Cu-700, Fe/Cu-800, and Fe/Cu-900 catalysts.

Catalyst	Fe/Cu-700	Fe/Cu-800	Fe/Cu-800
Fe (%)	**27.53**	**62.3**	**77.63**
Cu (%)	**1.47**	**2.23**	**2.27**

Table S4. ICP-OES quantification of Fe and Cu leaching concentrations in the reaction solution across four experimental groups and the corresponding metal content of the recovered Fe/Cu-800 catalyst before and after the reaction.

Fe/Cu-800	before	1	2	3	4	after
Fe	**62.3%**	**0.289 ppm**	**0.292 ppm**	**0.790 ppm**	**0.360 ppm**	**48%**
Cu	**2.23%**	**1.638 ppm**	**0.049 ppm**	**1.315 ppm**	**0.052 ppm**	**1%**

Table S5. Detailed information on TC degradation intermediates.

Number	Chemical Formula	Exact Mass	Molecular Weight	Proposed structure
TC	C22H24N2O8	444.15	444.44	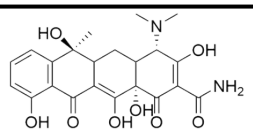
P2	C22H22N2O9	458.13	458.42	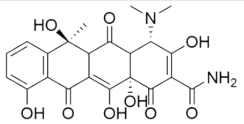
P3	C21H22N2O8	430.14	430.41	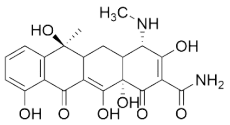
P4	C21H19NO7	397.12	397.38	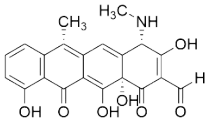
P5	C3H4O5	120.01	120.06	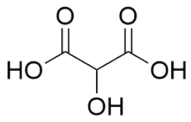
P6	C6H12O	100.09	100.16	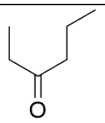
P7	C20H20N2O8	416.12	416.39	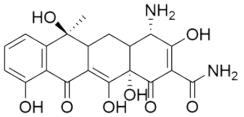
P8	C8H16O9	256.08	256.21	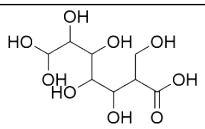
P9	C6H12O7	196.06	196.16	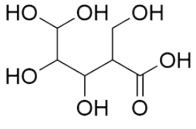
P10	C8H6O5	182.02	182.13	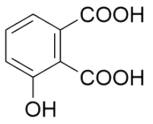
P11	C4H9NO4	135.05	135.12	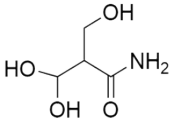

P12	C21H22N2O8	430.14	430.41	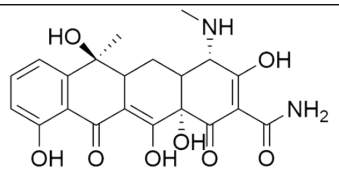
P13	C20H23NO8	405.14	405.40	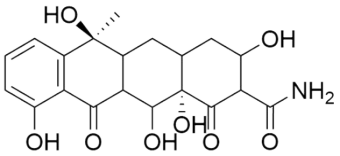
P14	C7H6O2	122.04	122.12	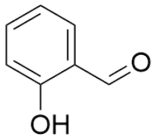
P15	C21H21NO7	399.13	399.4	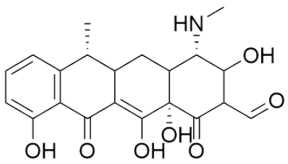
P16	C9H10O4	182.06	182.18	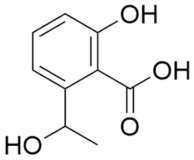
P17	C6H12O	100.09	100.16	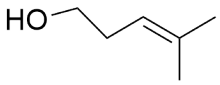
P18	C20H20N2O7	400.13	400.39	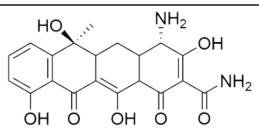
P19	C13H14O6	266.08	266.25	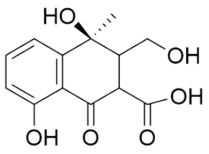
P20	C10H10O4	194.06	194.19	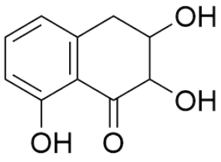

References

[1] Ke Zhang, Sha Kang, Ruige Jia, Chuanyi Wang, Unraveling the impact of Cu-loading in MIL-101(Fe) for markedly boosting photocatalytic PMS activation for TC degradation, Environ Res., 278,2025,121664.

[2] Qiang Cheng, Haotian Qin, Jiaxi Wu, Jingping Li, Kai Wang, Tailoring the structure of Fe_2TiO_5 via cobalt doping for efficient singlet oxygen production in persulfate-based tetracycline degradation, Colloid Surface A, 728, 2026,138762.

[3] Yanxia You, Lei Song, Yang Guo, Xuejun Zhang, Si Hu, Coupled homogeneous-heterogeneous Fenton-like system to highly efficiently degrade tetracycline in water at circumneutral pH: Mechanism and toxicity evaluation, J. Water Process Eng., 72, 2025, 107569.

[4] Activation of peroxymonosulfate by CoP@Co_2P heterostructures via radical and non-radical pathways for antibiotics degradation, Ceram. Int., 49, 2023, 16999-17007,

[5] Shichun Gu, Caiying Xia, Yapeng He, Hui Huang, Xue Wang, Core-shell Fe_3O_4@mesoporous carbon composite for tetracycline degradation via peroxymonosulfate activation, J. Solid State Chem., 352, 2025, 125614.

[6] Wang, Q.; Shi, Y.; Lv, S.; Liang, Y.; Xiao, P. Peroxymonosulfate activation by tea residue biochar loaded with Fe_3O_4 for the degradation of tetracycline hydrochloride: performance and reaction mechanism. RSC Adv., 11, 2021, 18525–18538.

[7] Tao, Yufang, Shenshen Sun, Yunzhen Hu, Shijie Gong, Shiyun Bao, Huihui Li, Xinyi Zhang, Zhe Yuan, and Xiaogang Wu. Activation of Peroxymonosulfate by Fe, O Co-Embedded Biochar for the Degradation of Tetracycline: Performance and Mechanisms, Catalysts 14, 2024, 556.

[8] Nguyen, The Luan and Tran, Hong Huy and Huynh, Tu Cam and Le, Khoa Tien and Cao. Harnessing potassium peroxymonosulfate activation of WO_3/diatomite composites for efficient photocatalytic degradation of tetracycline. RSC Adv., 2024, 14, 25019-25030.

[9] Liquan Wang, Ruyi Li, Yimin Zhang, Baohua Tu, Yuan Zhao, Ting Chen, Yuexiang Gao, Phosphorus doping to enhance the peroxymonosulfate activation efficiency of carbon nitride for degrading tetracycline, J. Water Process Eng., 54, 2023, 103916.

[10] Xueer Peng, Chenyang Zhou, Xuelian Li, Kai Qi, Lili Gao, Degradation of tetracycline by peroxymonosulfate activated with $Mn_{0.85}Fe_{2.15}O_4$-CNTs: Key role of singlet oxygen, Environ. Res., 227, 2023, 115750.

[11] Hao-Liang Jiang, Ming-Hui Li, Ling-Xi Zhao, Zhao-Xing Yan, Meng Xie, Jin-Ming Lin, Ru-Song Zhao, A novel oxygen vacancies enriched CoNi LDO catalyst activated peroxymonosulfate for the efficient degradation of tetracycline, J. Water Process Eng., 52, 2023, 103526.

[12] Chenglin Li, Dedong Sun, Hongchao Ma, Xinxin Zhang, Guowen Wang, Jun Hao, Enhanced peroxymonosulfate activation by $MoS_2/NiCo_2S_4$ composite catalyst for efficient elimination of tetracycline hydrochloride, J. Environ. Chem. Eng., 12, 1, 2024, 111900.

[13] Huan Deng, Yu Jin, Bojiao Yan, Yi Jiang, Shenggang Yang, Tiehong Song; Degradation of tetracycline by heat/peroxymonosulfate and ultrasound/peroxymonosulfate systems: performance and kinetics. Water Sci. Technol. 89, 2024, 421–433.